

Coupled equations for mass and momentum balance in a stream network: theoretical derivation and computational experiments

BY PAOLO REGGIANI¹, MURUGESU SIVAPALAN¹,
S. M. HASSANIZADEH² AND WILLIAM G. GRAY¹†

¹*Centre for Water Research, Department of Environmental Engineering,
University of Western Australia, 6907 Nedlands, Australia*

²*Section of Hydrology and Ecology, Faculty of Civil Engineering and Geosciences,
Delft University of Technology, PO Box 5048, 2600GA Delft, The Netherlands*

Received 24 February 2000; accepted 3 August 2000

In previous work by the authors a rigorous procedure for the derivation of global watershed-scale balance laws for mass, momentum, energy and entropy has been pursued. To complement these, a set of constitutive relations for the closure of the mass and momentum balance equations has also been derived, based on the exploitation of the second law of thermodynamics. In this paper these governing equations, including the constitutive relations, are rederived for the simpler case of the stream channel network of a natural watershed. The derived constitutive relationships for mass and force exchanges amongst channel reaches are physically consistent and thermodynamically admissible insofar as they respect physical constraints and keep the total entropy production of the system always positive. Next, the resulting system of coupled nonlinear ordinary differential equations are simultaneously solved for a natural watershed under realistic conditions. The numerical model presented permits the estimation of space-time fields of average velocity, storage and discharge within all reaches of the network tree during run-off events. The network response, as well as space-time fields of velocity and discharge, are computed for a number of rainfall events of different magnitude and different levels of network discretization. The nonlinearity of the response and the effects of different discretizations of the network are analysed in terms of computational experiments.

Keywords: channel network; balance equations; constitutive relationships; network routing; instantaneous unit response functions

1. Introduction

The purpose of this paper is to develop governing equations for the description of stream channel network responses. The governing equations are based on balances of mass and momentum, are formulated at the spatial scale of a reach, depend only on time, and can be employed for the prediction of space-time fields of average velocity and storage for each reach within the network.

† On leave from the Department of Civil Engineering and Geological Sciences, University of Notre Dame, Notre Dame, IN 46556, USA.

As pointed out by Gupta & Waymire (1998), any rigorous study of channel network response will remain incomplete without the incorporation of the balance of momentum, along with the mass balance into the set of governing equations. This fact has been contemplated within this paper by formulating global balance laws for mass and momentum for each reach and by supplying constitutive relationships which are necessary for the closure of the mass and force exchanges across the boundaries of the chosen control volume.

Generally, in the hydraulics literature, channel flow is described with the aid of the Saint-Venant equations. These constitute a set of conservation equations for mass and momentum, which have been averaged over the cross-section of the channel (as shown, for example, in Gray *et al.* (1993), Batchelor (1988) and Eagleson (1970)). The Saint-Venant equations depend explicitly on space and contain partial derivatives along the channel-axis. As such, they belong to the family of partial differential equations (PDEs). Over the last three decades, a rich literature has developed, where these equations have been solved by employing different numerical techniques (see Chow *et al.* (1988) for reference).

Our aim is to derive average balance equations for mass and momentum for a network, where the individual links serve as control volumes. The resulting equations thus depend only on time and belong to the family of ordinary differential equations (ODEs). In such an equation system, spatial variability in terms of hydraulic properties, geometry or rainfall input for individual reaches is taken into account. For each reach, these quantities are represented by their respective spatial averages.

The work presented here forms part of a broader, integrated modelling approach for the prediction of hydrological behaviour of general watersheds. The proposed method is physically based, involves the solution of watershed-scale governing equations, respects the presence of a stream channel network, and is parsimonious in terms of the required parameter values. The theoretical framework for the approach has been formulated in two recent publications by Reggiani *et al.* (1998, 1999). In the first paper, complete balance laws for mass, momentum, energy and entropy for an entire watershed, comprising unsaturated and saturated zones, two overland flow zones and the channel network zones, are formulated. These are obtained by first identifying a well-defined spatial region called the *representative elementary watershed* (REW) and respective sub-regions resembling the five flow domains, and by subsequently averaging the point-scale conservation equations over the volumes associated with these regions. In addition, the balance laws are also averaged over a characteristic time interval. Integration in time is important in the context of the integrated modelling framework, as it involves the aggregation of governing equations for flow processes operating over vastly different time scales.

The REW constitutes a fundamental building block for hydrological analysis, with the aid of which the watershed can be discretized into an interconnected set of entities where the stream channel network acts as a skeleton or organizing structure. The stream network associated with a watershed forms a binary tree structure consisting of nodes interconnected by channel reaches or links, as shown schematically in figure 1a for an ensemble of 13 reaches. The averaging procedure, carried out by Reggiani *et al.* (1998), has resulted in a set of coupled nonlinear ODEs which need to be solved to obtain flow rates (or velocities) and water depths (or storage) for the unsaturated and saturated zones, the overland flow zones and the channel network. Regional groundwater flow and its interaction with overland flow are also taken into account.

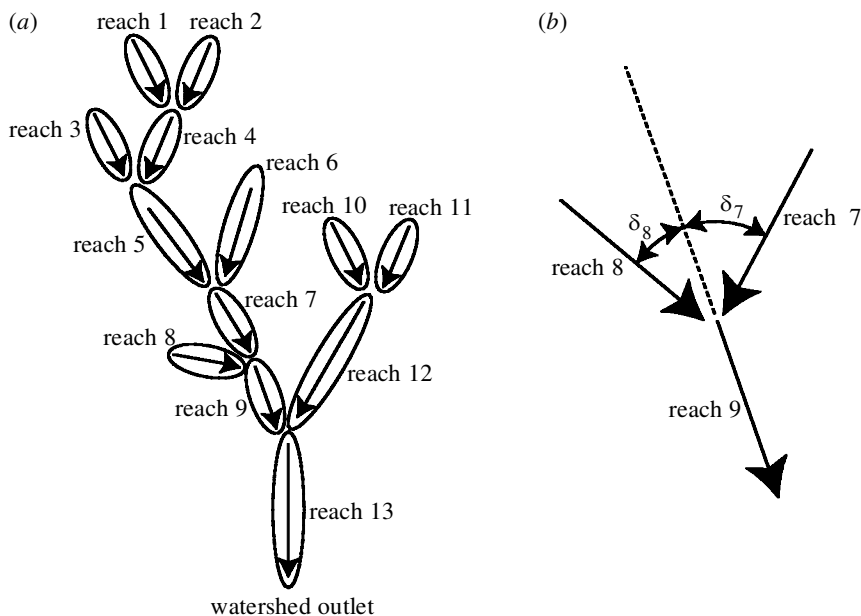


Figure 1. (a) Hierarchical arrangements of 13 reaches forming a channel network. (b) Detailed view of the confluence of two reaches.

However, the obtained governing equations are indeterminate (have more unknowns than equations) and contain terms of mass and force exchanges amongst various REWs and between various subregions within each REW. Appropriate constitutive relationships are needed for these exchange terms. A set of general constitutive relationships has been obtained by Reggiani *et al.* (1999) for an entire watershed, involving the use of the second law of thermodynamics as a constraint-type relationship. This approach for the derivation of constitutive relationships is known in the literature as the Coleman–Noll procedure (Coleman & Noll 1963) and has been previously applied in the field of porous media flow within the unsaturated and saturated zones (see, for example, Hassanizadeh & Gray 1990; Gray & Hassanizadeh 1991). The Coleman–Noll procedure provides a theoretically sound and systematic approach for tackling the closure problem.

This paper, however, focuses on the response of the channel network of a watershed only, and ignores the presence of the two subsurface flow zones and the overland flow zones. This is equivalent to the assumption that the entire volume of water associated with a single rainfall event is instantaneously accommodated in the channel network. The paper is structured into two main parts.

In the first part we state the governing balance laws for mass, momentum, energy and entropy for the individual reaches by following the procedure introduced by Reggiani *et al.* (1998, 1999). The first part also includes the derivation of *thermodynamically* admissible constitutive parametrizations through application of the Coleman–Noll method. By using the thermodynamic procedure, we avoid making *ad hoc* assumptions in the definition of force exchange terms. These are instead obtained naturally within the context of a single consistent procedure, which is founded on the use of a fundamental physical principle, the second law of thermodynamics.

In this fashion we are also able to clearly expose the hypotheses underlying common formulations involved in the description of channel network hydraulics, such as Chezy's law or the assumption of hydrostatic pressure distribution. The set of governing equations presented in this paper resemble a spatially integrated form of the *Saint-Venant* equations—a set of coupled nonlinear ODEs; these need to be solved simultaneously for all the reaches forming the network. For the complete specification of the governing equations, the balance equations and constitutive relations need to be supplemented with channel hydraulic geometries for all individual reaches. Here we specify these as functions of cumulative contributing watershed areas for the reaches. Expressions relating the various hydraulic geometries such as top width, average depth, and wetted perimeter to the upstream contributing watershed areas have been derived by Snell & Sivapalan (1995) using empirical *at-a-station* and *downstream* hydraulic geometry relationships introduced by Leopold & Maddock (1953). These relationships have been successfully tested in applied situations as shown in a recent paper by Naden *et al.* (1999). The contributing areas are also used here for the specification of steady-state initial conditions in the numerical solution of the governing equations.

In the second part we show that the proposed system of reach-scale conservation equations is indeed useful and has significant predictive power. We implement a numerical solver and perform response simulations for an actual watershed under various rainfall input scenarios and hypothetical boundary and initial conditions. The model allows the computation of space-time fields for discharges, storages and reach-average velocities in a straightforward manner. An additional aim of the numerical exercise is to explain how the geometrical and hydraulic information, necessary for the implementation of the model, can be obtained from digital maps and from regional hydraulic geometry coefficients and exponents, as suggested by Leopold & Maddock (1953). Finally, the nonlinearity of network response is discussed by comparing the estimated instantaneous unit response functions (IURFs) for rainfall inputs of varying depths, both for the main watershed as well as for a number of sub-watersheds.

2. Balance laws for mass and momentum and the second law of thermodynamics

The next three sections will present global balance equations for mass and momentum for a stream network, and the derivation of closure equations in the form of constitutive relations for exchanges amongst the reaches using the second law of thermodynamics. In all cases, for the sake of clarity and readability, we will present a summary of the results in the main text with the details relegated to an appendix. Note that the derivations presented here are a simplification of more complete derivations for the entire watershed system (including processes occurring within the hill-slopes). In this section, we present the conservation equations for mass and momentum and the second law of thermodynamics for an arbitrary reach of the network. Details are given in the appendix. The equations reported here refer to the i th reach within an ensemble of M reaches making up the whole network. See figure 1*a, b* for the arrangement of stream reaches and associated REWs, and figure 2 for a schematic view of a typical river reach.

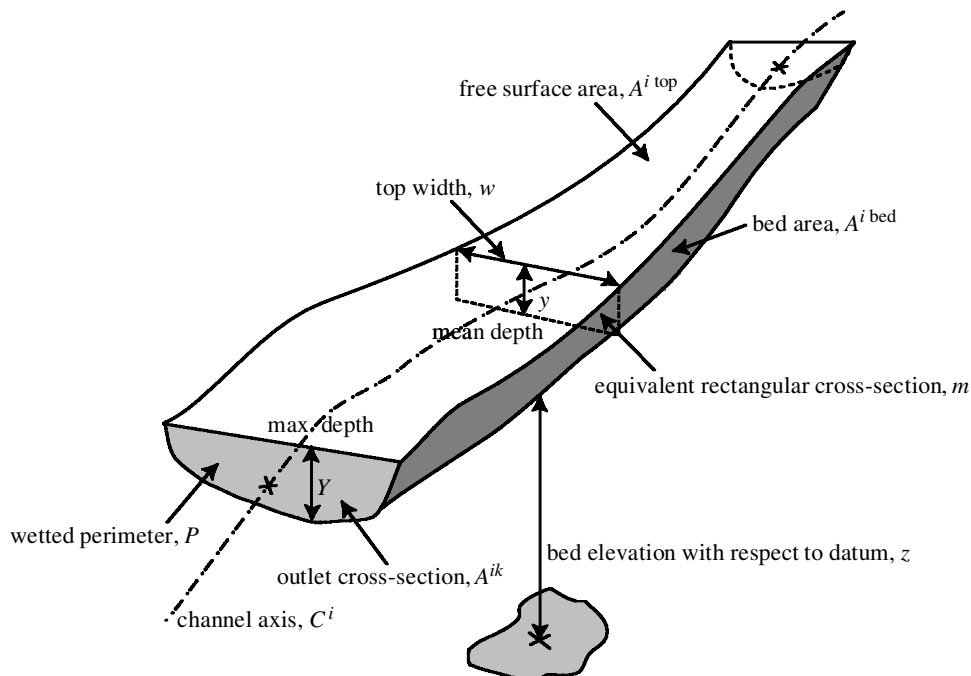


Figure 2. Schematic view of a single channel reach.

(a) Conservation of mass

By virtue of (A 1) and (A 6), the mass balance equation for the reach i is found to be

$$\frac{d}{dt}(\rho m^i l^i) = e^{i \text{ ext}} + \sum_{k \neq i} e^{ik} + e^{i \text{ top}}, \quad (2.1)$$

where $m^i[L^2]$ is the average cross-sectional area of the reach, $l^i[L]$ is the length of reach, and $\rho[M/L^3]$ is the (constant) density of water. The first term on the right-hand side, $e^{i \text{ ext}}$, is the outflow from the entire watershed. It is non-zero only for the one reach situated at the watershed outlet (e.g. reach 13 in figure 1a). The second term, $\sum_{k \neq i} e^{ik}$, is the sum of all exchanges with the adjoining reaches. For example, in the case of reach 4 in figure 1a, k assumes values 1 and 2, indicating the reaches converging at the inlet, and 5 indicating the reach following at the outlet. In the case of first-order streams, the summation includes only the reach following at the outlet (e.g. reach 1 in figure 1a is followed by reach 4). The last term, $e^{i \text{ top}}$, is the mass input (rainfall) or extraction (evaporation) on the channel free surface. We note that in (2.1) we have assumed that the channel bed is impermeable, and therefore $e^{i \text{ bed}} = 0$. Also, no lateral inflow into the channel from the adjacent land surfaces is considered.

(b) Conservation of momentum

The balance of momentum is obtained from (A 8) (see the appendix) by employing the product rule of differentiation to the left-hand side and exploiting the balance of

mass (2.1),

$$\rho m^i l^i \frac{d}{dt} \mathbf{v}^i - \rho m^i l^i \mathbf{g} = \mathbf{T}^{i \text{ ext}} + \sum_{k \neq i} \mathbf{T}^{ik} \cos \delta^{ik} + \mathbf{T}^{i \text{ bed}} + \mathbf{T}^{i \text{ top}}, \quad (2.2)$$

where δ^{ik} is the local angle of confluence between reaches i and k , as depicted in figure 1b. The first term on the right-hand side, $\mathbf{T}^{i \text{ ext}}$, is non-zero only for the outlet reach (reach 13 in figure 1a). It corresponds to the boundary force exerted at the outlet. The second term, $\sum_{k \neq i} \mathbf{T}^{ik} \cos \delta^{ik}$, is the sum of forces exchanged with the adjoining reaches k at the inlet and outlet sections. The third term, $\mathbf{T}^{i \text{ bed}}$, is the total friction force exchanged with the channel bed, while the last term, $\mathbf{T}^{i \text{ top}}$, is the sum of the pressure and viscous forces exchanged with the atmosphere on the channel free surface. This equation is vectorial and needs to be projected along the channel average direction by scalar multiplication with an appropriate unit vector. For this reason, we introduce an effective unit vector \mathbf{n}^i tangent to the channel bed of each reach. This vector will be employed to project (2.2) along the direction of flow and obtain scalar equations.

(c) Second law of thermodynamics

The second law of thermodynamics states that the entropy production of the entire system must always be non-negative. The second law of thermodynamics for the entire network has been obtained in Reggiani *et al.* (1999) and can be stated as

$$\begin{aligned} \theta L = & \sum_i \sum_{k \neq i} \left[\frac{p^k}{\rho} - \frac{p^i}{\rho} - g(z^k - z_0) + g(z^i - z_0) + \frac{1}{2}(v^{k,i})^2 \right] e^{ik} \\ & + \sum_i \sum_j [\mathbf{T}^{ij} - \boldsymbol{\Phi}^{ij}] \cdot \mathbf{v}^{j,i} + \sum_i [\rho g(z^i - z_0) + p^i] \dot{V}^i \geq 0, \quad j = k, \text{ bed, top}, \end{aligned} \quad (2.3)$$

where the vector $\boldsymbol{\Phi}^{ij}$ is defined as

$$\boldsymbol{\Phi}^{ij} = \int_{A^{ij}} \mathbf{n}^{ij} g(z - z_0) dA, \quad (2.4)$$

with z^i the elevation of the centroid of the reach, p^i the average pressure of the reach, V^i the volume occupied by the reach and z_0 a common reference elevation. Expression (2.3) indeed constitutes a minimum principle, as shown by Prigogine (1967) for closed thermodynamic systems. That is, at equilibrium, L is equal to zero. Thus, if we define a thermodynamic variable space Z_μ , within which L is defined, it follows that under conditions of thermodynamic equilibrium (i.e. at the origin of the variable space) L must reach an absolute minimum. The necessary and sufficient requirements for this condition to hold are that the first derivative of L with respect to Z_μ must be zero, i.e.

$$\left[\frac{\partial L}{\partial (Z_\mu)} \right]_e = 0, \quad (2.5)$$

and the norm of the second derivative, i.e.

$$\left\| \left[\frac{\partial^2 L}{\partial (Z_\mu) \partial (Z_\lambda)} \right]_e \right\|, \quad (2.6)$$

must be positive semi-definite.

3. Constitutive relationships

For the simulation of a flood wave travelling down a channel network, simultaneous solution of balance equations of mass (2.1) and momentum (2.2) for all M reaches is required. These balance equations, which have been presented in §2, contain a number of mass and momentum exchange terms (between an individual reach and its immediate environment, and between different reaches across their end sections) which are generally unknown. This represents a *closure* problem, and a common solution is to postulate appropriate constitutive relationships which relate each unknown exchange term to the *independent* variables chosen for the system. For the present problem, the independent variables will be the average cross-sectional area m^i and the average velocity \mathbf{v}^i , for each reach. Thus we propose the following dependencies

$$\left. \begin{array}{l} \text{mass exchange: } e = e(m^i, \mathbf{v}^i), \\ \text{momentum exchange: } \mathbf{T} = \mathbf{T}(m^i, \mathbf{v}^i). \end{array} \right\} \quad (3.1)$$

Since thermal problems are not considered in the present work, constitutive parametrizations are not being sought for the closure for eventual heat exchange terms among reaches and the surrounding environment. This represents a considerable simplification of the problem. The procedure for the derivation of constitutive relationships is based on the method pioneered by Coleman & Noll (1963), which is based on the exploitation of the entropy inequality (2.3) and has been previously used by Hassanizadeh & Gray (1990) in porous media theories and Reggiani *et al.* (1999) in watershed theories.

(a) *The entropy inequality at equilibrium*

According to the second law of thermodynamics, the entropy production of the entire system is always non-negative and will be zero only at thermodynamic equilibrium. For the network made up of an ensemble of reaches, a situation of thermodynamic equilibrium can be defined as the status of zero entropy production. We observe that there are different possibilities for the definition of equilibrium within a reach. In general, the production of entropy L is zero under no-flow conditions. In the case of steep channels, for example, no-flow conditions can only be reached when the reach is dry. In the case of almost flat channels, equilibrium can be defined as when there is stagnant water within the reach. Such a definition of equilibrium requires the following assumption, which is commonly referred to as the Saint-Venant hypothesis (see, for example, Cunge *et al.* 1980).

Assumption 3.1 *The slope of the bed is small, so that the cosine of the angle between the bed and the horizontal is essentially 1.*

Assumption 3.1 allows us to define equilibrium as the condition of a horizontal free surface within a reach. In such a situation, the forces acting are balanced and the following set of variables becomes zero for all reaches:

$$(Z_\mu)_i = [\mathbf{v}^i, \dot{V}^i, e^{ik}] = 0. \quad (3.2)$$

Therefore, at equilibrium, none of the reaches is subject to expansion or reduction of their respective storage volumina V^i and all reaches are at a common temperature θ . Furthermore, the velocities and mass exchange terms are also zero. Next, we take the

derivative of the entropy inequality (2.3) with respect to the variables listed in (3.2) and impose condition (2.5). The result of this operation yields a series of equilibrium conditions. From the first line of (2.3), we obtain that

$$p^i - \rho g(z^i - z_0) = p^j - \rho g(z^j - z_0), \quad (3.3)$$

i.e. the total pressure heads across the interface A^{ij} , defined in the appendix, must be equal. The differentiation of the second line with respect to \mathbf{v}^i yields

$$\mathbf{T}^{ij}|_e - \Phi^{ij} = 0, \quad j = k, \text{bed, top}, \quad (3.4)$$

where the vector Φ^{ij} is defined through (2.4). From the last term of (2.3), we obtain the equilibrium condition

$$p^i + \rho g(z^i - z_0) = 0. \quad (3.5)$$

Combination of (3.4) and (3.5), by eliminating the reference elevation, leads to the equilibrium expression for the momentum exchange terms

$$\mathbf{T}^{ij}|_e = \int_{A^{ij}} \mathbf{n}^{ij} \cdot [-p^i + \rho g(z - z^i)] dA, \quad j = k, \text{bed, top}. \quad (3.6)$$

Equation (3.6) can be used for two different purposes: either to evaluate $\mathbf{T}^{ij}|_e$, if the pressure is known, or to calculate p^i if $\mathbf{T}^{ij}|_e$ is known. For example, at equilibrium, in the absence of frictional effects, the pressure on the channel surface is atmospheric, i.e. $\mathbf{T}^{i \text{top}}|_e = 0$. Consequently, equation (3.6) yields

$$p^i = \rho g(z^{i \text{top}} - z^i), \quad (3.7)$$

where we recall that $z^{i \text{top}}$ is the average elevation of the free surface of the reach and z^i is the elevation of its centroid. If we denote the average elevation of the bed with $z^{i \text{bed}}$ and the average water depth with y^i , we can substitute in (3.7) and obtain an approximate expression for the average pressure,

$$p^i = \rho g[(y^i + z^{i \text{bed}}) - (\frac{1}{2}y^i + z^{i \text{bed}})] = \frac{1}{2}\rho g y^i. \quad (3.8)$$

The pressure is equivalent to the average hydrostatic pressure and can be used in (3.6) for the evaluation of the force acting on the channel bed under equilibrium conditions,

$$\mathbf{T}^{i \text{bed}}|_e = \int_{A^{i \text{bed}}} \mathbf{n}^{i \text{bed}} \cdot [-p^i + \rho g(z - z^i)] dA. \quad (3.9)$$

For the equilibrium forces acting on the end sections of the reach (inlet and outlet) we invoke assumption 3.1, which allows us to state that the elevation of the centroid of the cross-sectional area A^{ik} , z^{ik} is comparable with the the elevation of the reach centroid z^i ,

$$z^{ik} \approx z^i. \quad (3.10)$$

From (3.6), we subsequently obtain an expression for the force acting on the cross-section at equilibrium,

$$\mathbf{T}^{ik}|_e = -p^i A^{ik} \mathbf{n}^{ik}. \quad (3.11)$$

(b) *Non-equilibrium parametrization of the momentum exchange terms*

In (3.9) and (3.11) we have obtained expressions for the forces under equilibrium conditions, which are attributable to the pressure forces only. Under non-equilibrium conditions, viscous forces appear next to the pressure forces, which need to be properly accounted for. Therefore, we propose to write the momentum exchange terms as the sum of two parts, the sum of all equilibrium forces acting on the reach, $\mathbf{T}^{ik}|_e$, $\mathbf{T}^{i \text{bed}}|_e$ and $\mathbf{T}^{i \text{top}}|_e$, and a non-equilibrium part expressed as a function of the velocity, which becomes zero at equilibrium,

$$\mathbf{T}^{ij} = \sum_{j \neq i} \mathbf{T}^{ij}|_e + \bar{\boldsymbol{\tau}}^i, \quad j = k, \text{bed, top.} \quad (3.12)$$

The equilibrium part given by the pressure forces has been obtained in (3.9) and (3.11). The non-equilibrium component $\bar{\boldsymbol{\tau}}^i$ is derived through a second-order Taylor series expansion of the forces in terms of the velocity around the sum of their equilibrium expressions $\sum_{k \neq i} \mathbf{T}^{ik}|_e$,

$$\bar{\boldsymbol{\tau}}^i = -\mathbf{v}^i \cdot \mathbf{R}^i - |\mathbf{v}^i| \mathbf{U}^i \cdot \mathbf{v}^i, \quad (3.13)$$

where \mathbf{R}^i and \mathbf{U}^i are tensors. The second-order dependence on velocity is postulated since, for channel flows, experimental observations suggest that the friction forces at the local point scale depend on the square of the velocity. This fact is evident from well-known formulations such as the Chezy & Manning equations. Here we neglect the first-order term in (3.13) and project the equation along the effective direction of flow through scalar multiplication by the unit tangent vector to the channel bed \mathbf{n}^i ,

$$\bar{\boldsymbol{\tau}}^i \cdot \mathbf{n}^i = -|\mathbf{v}^i| \mathbf{U}^i \cdot \mathbf{v}^i \cdot \mathbf{n}^i, \quad (3.14)$$

obtaining a scalar expression,

$$\bar{\tau}^i = -U^i v^i |v^i|, \quad (3.15)$$

where U^i is a reach average hydraulic friction coefficient for the corresponding reach. In the present application, we assume that U^i is given by

$$U^i v^i |v^i| = P^i l^i \tau_0^i, \quad (3.16)$$

where P^i is the average wetted perimeter of the reach, l^i is the reach length and τ_0^i is the average shear stress acting on the channel bottom, given by

$$\tau_0^i = \frac{1}{8} \rho \xi^i v^i |v^i|, \quad (3.17)$$

yielding

$$U^i = \frac{1}{8} \rho P^i l^i \xi^i, \quad (3.18)$$

with ξ^i being the reach-average Darcy–Weisbach friction factor. For fully turbulent flow, ξ^i can be related to the average roughness height $\epsilon^i[L]$ and the average maximum flow depth $Y^i[L]$ of the reach, as established by Keulegan (1938) and extended by Bray (1979),

$$\frac{1}{\sqrt{\xi^i}} \approx 0.248 + 2.28 \log_{10} \left[\frac{Y^i}{\epsilon^i} \right]. \quad (3.19)$$

Note that the assumption that the tensor \mathbf{R}^i in (3.13) is zero is merely a convenient assumption which conforms to common hydraulic practice, and can be relaxed, if needed, especially when there is empirical evidence to warrant it.

(c) Linearization of the mass exchange terms

The mass exchange terms across the reach end sections are unknown quantities of the problem. From the entropy inequality (2.3), a linearization of the mass exchange terms as functions of the average velocities within the adjacent sub-regions is suggested,

$$e^{ik} = -\mathcal{B}^{ik} \frac{1}{2} A^{ik} (\mathbf{v}^i + \mathbf{v}^k) \cdot \mathbf{n}^{ik}, \quad (3.20)$$

where the vector \mathbf{n}^{ik} represents the unit normal to the cross-sectional area A^{ik} . The coefficients \mathcal{B}^{ik} are correction factors for the respective mass exchange terms and are defined as follows:

$$\mathcal{B}^{ik} = \rho \left(\frac{m^i}{m^k} \right) \quad (3.21)$$

for the two inlet sections and

$$\mathcal{B}^{ik} = \rho \left(\frac{m^k}{m^i} \right) \quad (3.22)$$

at the downstream cross-section. We observe that the ratio of the cross-sections for the two subsequent reaches varies approximately between 0.5 and 1.5. From a numerical perspective, this parametrization diffuses differences in storage among the reaches by increasing the outflow rate if the storage of the downstream reach decreases and by reducing it if the storage of the downstream reach increases. In this fashion, this formulation causes a dynamic smoothing of the cross-sectional areas of adjacent reaches. A similar equation may be used for the mass exchange $e^{i \text{ext}}$, at the watershed outlet (non-zero only for the reach situated at the outlet),

$$e^{i \text{ext}} = -\mathcal{B}^{i \text{ext}} \frac{1}{2} A^{i \text{ext}} (\mathbf{v}^i + \mathbf{v}^{\text{ext}}) \cdot \mathbf{n}^{i \text{ext}}, \quad (3.23)$$

where

$$\mathcal{B}^{i \text{ext}} = \rho \left(\frac{m^i}{m^{\text{ext}}} \right) \quad (3.24)$$

and \mathbf{v}^{ext} and m^{ext} are assumed to be known. For example, in the case of a river flowing into a lake or sea, m^{ext} is known and \mathbf{v}^{ext} may be set equal to zero.

4. Parametrized equations

Final parametrized balance equations for mass and momentum are obtained by substituting the constitutive relationships (3.12) and (3.15) for the momentum exchange term and (3.20) for the mass exchange term into (2.1) and (2.2), respectively. These are presented below. The system of parametrized balance equations, reported here for an ensemble of M reaches, form a system of $2M$ nonlinear coupled ODEs in $2M$ variables m^i and \mathbf{v}^i . Additional parameters required for the solution of the system of equations are the roughness height ϵ^i and the geometric variables such as the length l^i for every reach. The numerical solution of these coupled balance equations will be reported in the sections that follow.

(a) Conservation of mass

The parametrized form of the conservation equation of mass is obtained by substituting the mass exchange terms (3.20) and (3.23) into (2.1). The result is

$$\underbrace{\frac{d}{dt}(\rho m^i l^i)}_{\text{storage}} = \sum_{k \neq i} \underbrace{\pm \mathcal{B}^{ik} \frac{1}{4}(m^i + m^k)(v^i + v^k)}_{\text{inflow, outflow among reaches}} - \underbrace{\mathcal{B}^{i \text{ext}} \frac{1}{4}(m^i + m^{\text{ext}})(v^i + v^{\text{ext}})}_{\text{watershed outflow}}, \quad (4.1)$$

where, once again, the last term is non-zero only for the watershed outlet reach (e.g. reach 13 in figure 1a). The sign of the first term on the right-hand side is positive for inlet sections (mass source) and negative for outlet sections (mass sink). We observe that the conservation of mass for the reach is dependent on the velocities and cross-sectional areas of the adjacent reaches.

(b) Conservation of momentum

The conservation equation of momentum is vectorial. Before obtaining scalar equation through projection, we first replace the momentum exchange terms in (2.2) by the sum of the equilibrium forces and the non-equilibrium component (3.13),

$$\rho m^i l^i \frac{d}{dt} \mathbf{v}^i - \rho m^i l^i \mathbf{g} = \mathbf{T}^{i \text{ext}} + \sum_{k \neq i} \mathbf{T}^{ik}|_e \cos \delta^{ik} + \mathbf{T}^{i \text{bed}}|_e - |\mathbf{v}^i| \mathbf{U}^i \cdot \mathbf{v}^i. \quad (4.2)$$

Next, we carry out a scalar multiplication of (4.2) with the effective unit vector \mathbf{n}^i tangent to the channel bed. In addition, we make a further assumption, which can be seen as a corollary of assumption 3.1.

Assumption 4.1 *The component of the bed surface normal to \mathbf{n}^i is negligible,*

$$\mathbf{n}^{i \text{bed}} \cdot \mathbf{n}^i \approx 0. \quad (4.3)$$

The final parametrized form of the conservation equation of momentum is

$$\underbrace{(\rho m^i l^i) \frac{d}{dt} v^i}_{\text{inertia}} = \underbrace{\rho g m^i l^i \sin \gamma^i}_{\text{gravity}} - \underbrace{\frac{1}{8} \rho P^i \xi^i v^i |v^i|}_{\text{Chezy resistance}} \pm \underbrace{\sum_{k \neq i} \frac{1}{4} \rho g y^i (m^i + m^k) \cos \delta^{ik}}_{\text{pressure forces exchanged across end sections}} - \underbrace{\frac{1}{4} \rho g y^i (m^i + m^{\text{ext}})}_{\text{pressure force at watershed outlet}}, \quad (4.4)$$

where the sign of the second to last term is positive on the inflow sections and negative on the outflow section of the reach. The angle γ^i is the average slope for the reach, to be obtained from elevation maps, while m^{ext} is imposed according to the boundary conditions. The angle δ^{ik} of the confluence of two reaches, for the steep watershed used in the following application, is only *ca.* 20°, yielding $\cos \delta^{ik} \approx 1$, and can thus be removed without loss of accuracy.

It is reassuring to observe that (4.4), which has been derived using the systematic approach presented in this paper, resembles an integrated form of the Saint-Venant momentum equation for a series of zero-dimensional interconnected channel reaches, after channel curvature effects have been neglected. In the case of steep channels, the pressure terms are negligible relative to the gravity term.

(c) *Residual entropy inequality*

Substitution of the parametrized mass and momentum exchange terms into the entropy inequality (2.3) yields the following residual entropy production for the network:

$$\begin{aligned} \theta L = & \sum_i \sum_{k \neq i} \frac{1}{4} \mathcal{B}^{ik} (v^i + v^k) (m^i + m^k) g \left[\frac{1}{2} (y^k - y^i) + (z^i - z_0) - (z^k - z_0) \right] \\ & - \sum_i \sum_{k \neq i} \frac{1}{8} \mathcal{B}^{ik} (v^i + v^k) (m^i + m^k) (v^i)^2 + \sum_i \frac{1}{8} \rho P^i l^i \xi^i |v^i| (v^i)^2 \\ & \pm \sum_i \sum_{k \neq i} \rho g \frac{1}{2} y^i (m^i + m^k) v^i + \sum_i \rho g [z^i - z_0 + \frac{1}{2} y^i] \dot{V}^i \geq 0. \end{aligned} \quad (4.5)$$

The sign of the second last term is negative for inlet sections and positive for the outlet sections of each reach. We can easily verify that conditions (2.5) and (2.6) are always satisfied for the proposed parametrizations. This will be further confirmed using numerical estimates of residual entropy production for a number of rainfall-run-off events which will be simulated as part of the modelling exercise presented in § 6.

(d) *Geometric considerations*

Equations (4.1) and (4.4) complete the specification of the governing equations for the solution of the network routing problem. The solution of these equations requires the specification of additional geometric relationships to overcome a deficit of $3M$ unknowns with respect to the number of available equations. For example, the solution of (4.4) requires knowledge of the wetted perimeter P^i and the average mean depth y^i . The average maximum depth Y^i of the reach is needed to estimate the friction in (3.19). These geometric properties of the channel network can be expressed in terms of the main dependent variables m^i and v^i in the balance equations of mass and momentum.

However, the relationships between the dependent variables and the independent variables are not constitutive relations *per se* to be derived using thermodynamic considerations, but form part of the problem specification. In general, these can be derived based on analyses of field measurements. Since our focus here is mainly on an illustration of a modelling framework based on the derived balance equations, following Snell & Sivapalan (1995), we estimate these using a combination of the universal *at-a-station* and *downstream* hydraulic geometry relationships developed empirically by Leopold & Maddock (1953). These relationships allow us to express the average cross-sectional velocity, the top width and the average flow depth for a given stream reach as power laws of the discharge $D^i = m^i v^i$. Strictly speaking, they are valid under steady-state conditions but are in fact applied to a non-steady situation. These relationships have been successfully employed for real-world watershed situations, as shown in a recent paper by Naden *et al.* (1999).

The average top width w^i , average flow depth y^i and v^i for any given reach in time (*at-a-station*) or along the network at a given point in time (*downstream*) can

thus be expressed as power laws of m^i and v^i ,

$$w^i = a(m^i v^i)^b, \quad (4.6)$$

$$y^i = c(m^i v^i)^f, \quad (4.7)$$

$$v^i = k(m^i v^i)^n. \quad (4.8)$$

The scaling coefficients a , c and k are functions of position and thus vary from reach to reach. The variability between the reaches is strongly dependent on upstream contributing watershed area, and in this paper is assumed to be governed by Leopold & Maddock's *downstream* hydraulic geometry relationships. Details of the derivations are shown by Snell & Sivapalan (1995), and are omitted here in the interest of brevity. On the other hand, the exponents b , f and n are independent of space and time. The coefficients and exponents of the hydraulic geometry relationships can be evaluated from field data for any study region; in this paper, for illustration, we use indicative values suggested from the literature.

It can be shown that the maximum depth Y^i *at-a-station* is related to the mean depth y^i via the following relationship:

$$Y^i = y^i(1 + f/b). \quad (4.9)$$

The *at-a-station* wetted perimeter P^i can be derived by a line integration across the top width of the channel,

$$P^i = 2 \int_0^{Y^i} \left[1 + \frac{1}{4} \left(\frac{dw}{dy} \right)^2 \right]^{0.5} dy, \quad (4.10)$$

where w and y are two integration variables ranging between 0 and the average top width w^i , and between 0 and the average maximum depth of the reach Y^i , respectively. The above integral cannot be obtained in closed form and thus needs to be evaluated numerically.

5. Model data acquisition for a natural watershed

The network response model was applied to the 17 km² experimental watershed Coweeta, situated in the Appalachian mountains, North Carolina, in the eastern United States. For this watershed a 200 × 200 digital elevation map (DEM) with a pixel size of 30 × 30 m was available and was used to extract the stream network and associated sub-watershed areas using the DEM analysis software GMORF (for details, see Snell 1996). The algorithms in GMORF are based on the work pioneered by O'Callaghan & Mark (1984) and Band (1986). The analysis is performed by computing the steepest gradient and aspect for every pixel of the map. Within this framework, the extent of areas which contribute to the flow at any point of the land surface can be analysed.

A channel network is defined as consisting of those pixels which have at least a certain converging or accumulated *threshold contributing area*. The contributing area can be identified by a given number of pixels which are connected in terms of slope and aspect with the pixel under examination. Once a *threshold area* has been chosen, the ensemble of all interconnected pixels with an accumulated area greater than or equal to the threshold area represent the channel network. The

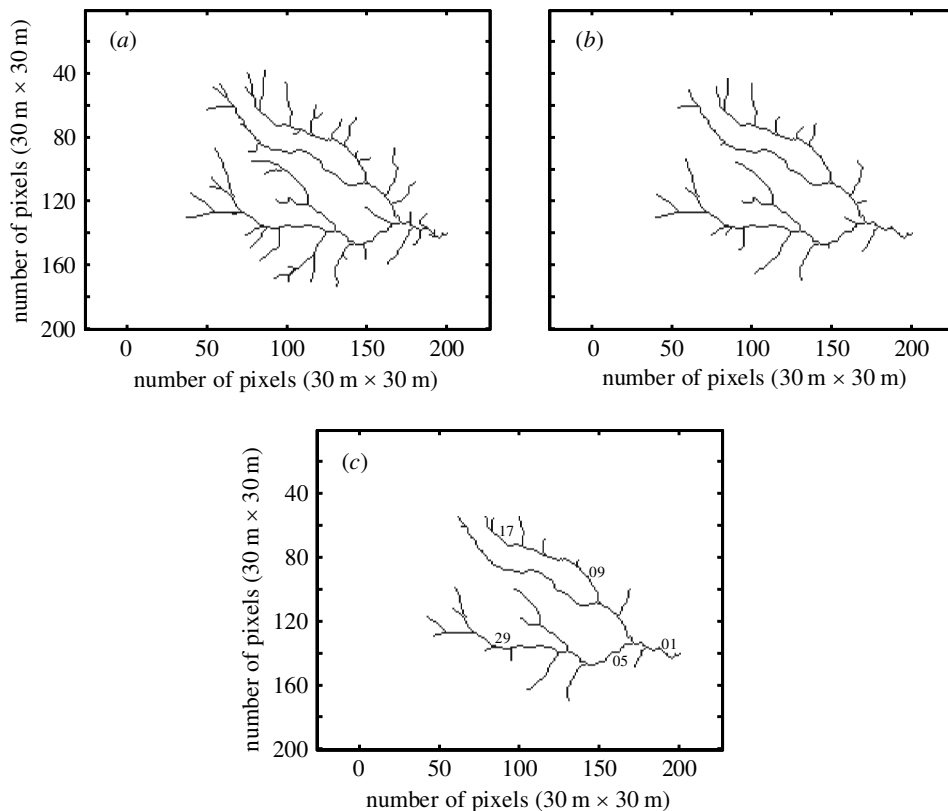


Figure 3. Channel network for the Coweeta watershed extracted with threshold areas of 100, 200 and 300 pixels ($30 \times 30 \text{ m}^2$) for parts (a), (b) and (c), respectively. (a) 87 reaches, (b) 49 reaches and (c) 37 reaches.

extracted network can subsequently be broken down into a number of M reaches, defined as the ensemble of network pixels connecting two nodes within the network. The streams are classified as *first order* if they are at the outer end of the network or *higher order* (Horton–Strahler network ordering system (Strahler 1964)) when situated between two internal nodes. The outlined analysis has been performed on the above DEM by imposing threshold areas of 100, 200 and 300 pixels, respectively. The projections of the obtained networks onto the horizontal plane are shown in figure 3a–c. The total number of reaches M for the three cases are found to be 87, 49 and 37. The respective values of the drainage densities are 2.13 , 1.56 and 1.29 km^{-1} . More geometric information can easily be extracted from the DEM analysis. For example, we obtain the slope γ^i , the length l^i , the sub-watershed area S^i , the total upstream contributing area S and the average elevation $z^i - z^0$ of the i th reach with respect to a datum.

With respect to hydraulic geometry, values for the coefficients and exponents needed are adopted from the literature (for reference, see Mosley 1992). The selected values for the parameters are listed in table 1. The units of the parameters are such that the top width and mean depth will be in metres (m), while the velocity is in m s^{-1} . We note that the scaling coefficients a , c and k for the *at-a-station* hydraulic

Table 1. *Hydraulic geometry parameter values*

parameter	value
at-a-station width exponent, b	0.26
at-a-station depth exponent, f	0.40
at-a-station velocity exponent, n	0.34
downstream width exponent, b	0.5
downstream depth exponent, f	0.4
downstream velocity exponent, n	0.1
downstream width coefficient, a	7.09
downstream depth coefficient, c	0.23
downstream velocity coefficient, k	0.61

geometry vary with total upstream contributing area S for each reach and can be estimated through appropriate expressions reported in Snell & Sivapalan (1995).

The roughness height ϵ for the various reaches has been generally observed (see, for example, Hack 1957) to increase from the flat high-order reaches with near-zero slopes in proximity to the outlet to higher values for the steep low-order reaches further upstream. Therefore, we employ a scaling approach where values for the roughness height are assigned to each reach based on the upstream contributing area relative to each reach,

$$\epsilon^i = d_\epsilon S^{q_\epsilon}, \quad (5.1)$$

where d_ϵ and q_ϵ are an appropriate scaling coefficient and exponent, respectively. The resulting values of the roughness height vary from 40 mm in the downstream reaches up to values of 200 mm in the first-order branches, with contributing areas ranging from the entire watershed area at the outlet to the chosen threshold area for first-order reaches. These considerations allow the evaluation of d_ϵ and q_ϵ .

6. Solution of the governing equations and discussion of results

For a network comprising M reaches, the governing equations consist of $2M$ coupled nonlinear ODEs; the mass and momentum equations for the each reach are (4.1) and (4.4), respectively. For the solution of the system, we have adopted a numerical algorithm presented by Press *et al.* (1992). The algorithm is based on the Runge–Kutta integration method, supplemented with adaptive step-size control. This control procedure allows one to monitor the local truncation error at every time-step. A tolerance based on the required accuracy can be specified; the algorithm then chooses a time step size which keeps the local truncation error within the desired limit. The estimation of the truncation error is performed by computing the difference between the solution obtained by a fifth-order Runge–Kutta formula and an embedded fourth-order formula, estimated using Cash–Karp (Cash & Karp 1990) parameter values. In order to keep the errors within desired bounds, the step size has to be adjusted at every iteration according to the requirements of the ‘worst offender’ within the set of $2M$ differential equations.

(a) *Implementation of initial and boundary conditions*

The specification of initial conditions requires the assignment of an initial velocity v_0^i and an initial average cross-sectional area m_0^i , for every reach at the beginning of the simulation. All results presented in this paper are for the response of the watershed to an instantaneous pulse of rainfall of specified depth falling over the watershed area, and all the rain water from this pulse is assumed to reach the stream network instantaneously.

Independent of the instantaneous injection of rainfall, a constant steady-state base-flow component is assumed in the network, which bears a steady-state cross-sectional area m_b^i for the k th reach. The cross-sectional area is calculated by applying a constant steady recharge rate $I_b = 1.0 \text{ mm h}^{-1}$ across the entire watershed, a background contribution which continues even after the rainfall injection. The recharge rate I_b , multiplied by the total upstream contributing area S for the reach, yields a steady-state discharge D_b^i . The area m_b^i is obtained by evaluating the steady-state base-flow velocity v_b^i from the hydraulic geometry relationship (4.8) and subsequently dividing D_b^i by the velocity v_b^i ,

$$m_b^i = D_b^i / v_b^i. \quad (6.1)$$

Now, given that an instantaneous rainfall of depth $J[L]$ is dumped over the watershed, the corresponding volume of water injected into the i th reach can be estimated by multiplying the local sub-watershed area S^i associated with that reach (different from the total contributing area up to the reach, S) by the rainfall depth J . Thus the initial volume V_0^i of water in the reach will be the sum of the above volume and the volume of water already in the reach due the prevailing base-flow, namely, $m_b^i \cdot l^i$. The initial average cross-sectional area m_0^i is subsequently obtained by dividing V_0^i by the length of the reach l^i ,

$$m_0^i = \frac{V_0^i}{l^i} = \frac{JS^i}{l^i} + m_b^i. \quad (6.2)$$

Once m_0^i is known, the initial velocity v_0^i can be evaluated, assuming steady-state conditions, from the hydraulic geometry relationship (4.8).

The boundary conditions for the mass and momentum balance equations at the watershed outlet are implemented by specifying the velocity v^{ext} and the cross-sectional area m^{ext} in (4.1) and (4.4). For the watershed under consideration, we specify at every time-step m^{ext} to be equal to m^i and v^{ext} to v^i of the watershed outlet reach (i.e. reach 1 in figure 3c). By implementing the boundary condition in this way, we exclude the flow within the network from being influenced by downstream conditions, which is reasonable for the steep watershed chosen in the present application. We emphasize that different boundary conditions could have been chosen for the case where the watershed outlet, for example, coincides with a water body with a constant or oscillating free surface (e.g. lake, artificial reservoir, sea).

(b) *Results and discussion*

This paper focuses on stream network response, and in the absence of models of hill-slope response, it is difficult to compare the results with field observations. For

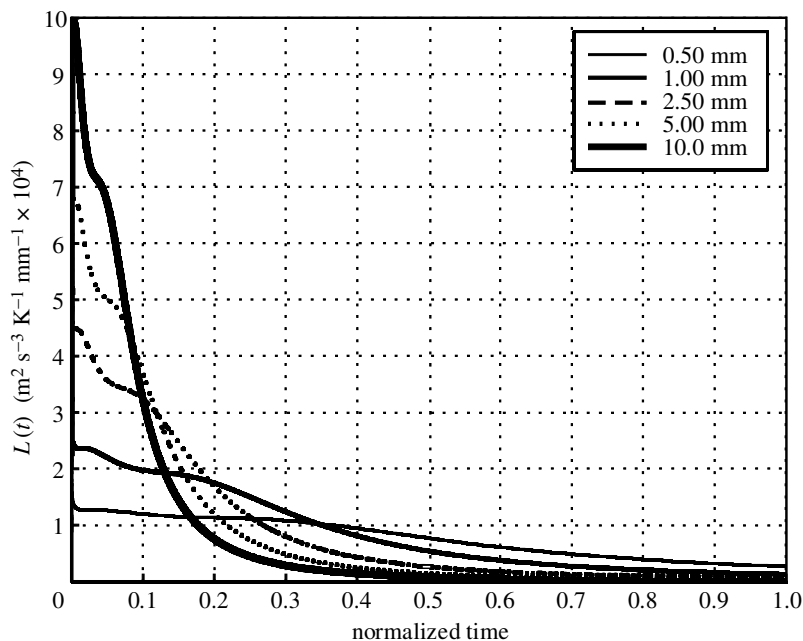


Figure 4. Entropy production versus time for the watershed in figure 3c during five different events, 37 reaches.

this reason, only hypothetical results are presented, for an actual stream network but with realistic initial and boundary conditions, and rainfall inputs. The motivation is to illustrate the functioning of the network response, and to interpret the model results with insights gained from the physics represented in the balance equations. More realistic results of catchment response will be presented in future work using models of hill-slope response which are based on rigorous balance laws derived by Reggiani *et al.* (1989, 1999).

The results presented here are from five different model simulations of the response of the watershed to instantaneous inputs of rainfall with varying rainfall depths J equal to 10.0, 5.0, 2.5, 1.0 and 0.5 mm. The events are equivalent to Dirac- δ type mass injections into the network, at simulation time $t_0 = 0$, and proportional to the area of the sub-watersheds associated with each reach. The simulations were carried out for three different discretizations of the watershed and network, resulting in networks comprising a number M of 87, 49 and 37 reaches, as shown in figure 3a-c. All simulations were continued for a period of 3.33 h (12×10^3 s). The results are interpreted in separate sections based on the respective figures.

(i) *Entropy production (figure 4)*

At the outset we wanted to verify, using the numerical model, that the constitutive parametrizations developed satisfy the second law of thermodynamics, at all times and under all conditions. For this reason, the rate of entropy production L as given by (4.5) was estimated over the course of the simulations. Representative results are given in figure 4 for the network shown in figure 3c ($M = 37$), for the five instantaneous rainfall events. Note that the net rate of entropy produc-

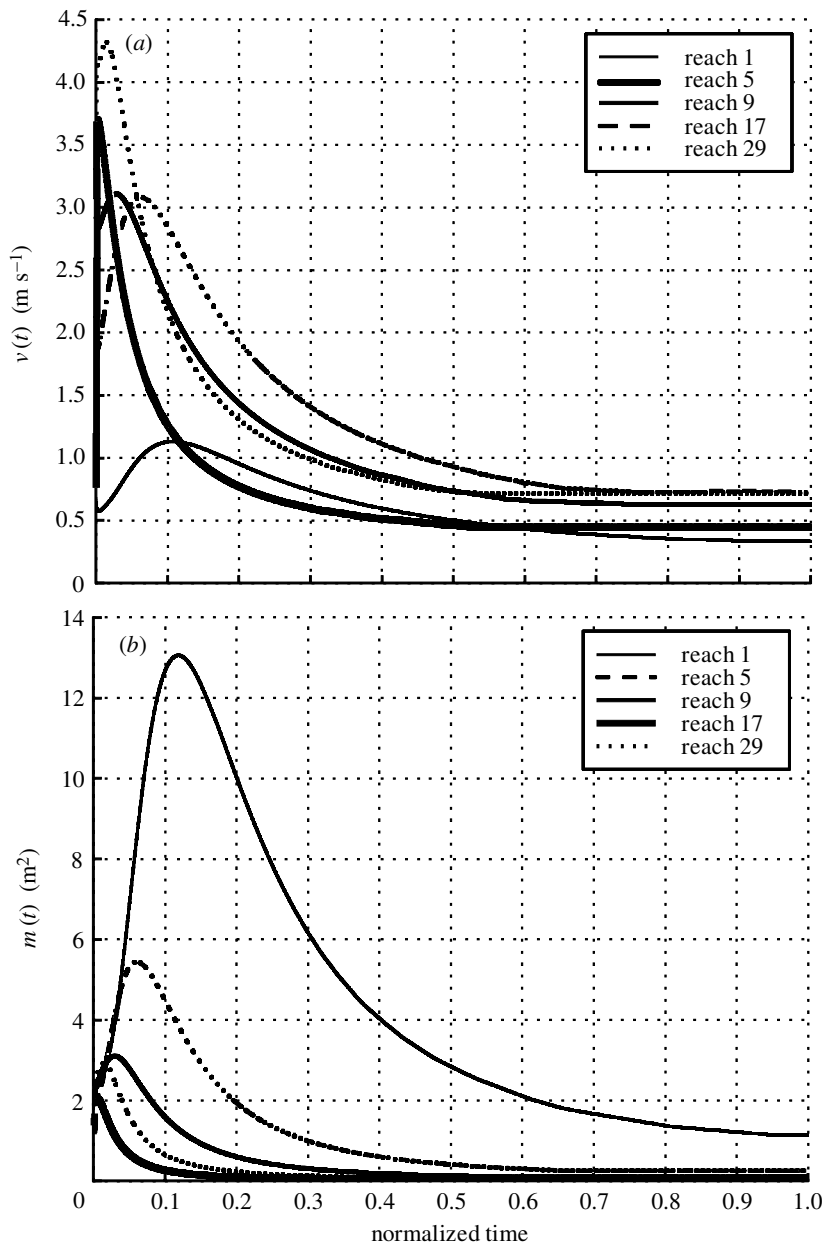


Figure 5. (a) Average velocity versus time for reaches 1, 5, 9, 17 and 29 indicated in figure 3c. (b) Average cross-sectional area versus time for reaches 1, 5, 8, 17 and 29 indicated in figure 3c.

tion has been divided by the constant density of the water and is normalized again by the rainfall depth J . It can be seen that the entropy production does indeed remain always non-negative, as required by the second law of thermodynamics. This confirms that the assumed constitutive relationships respect the imposed thermodynamic constraints.

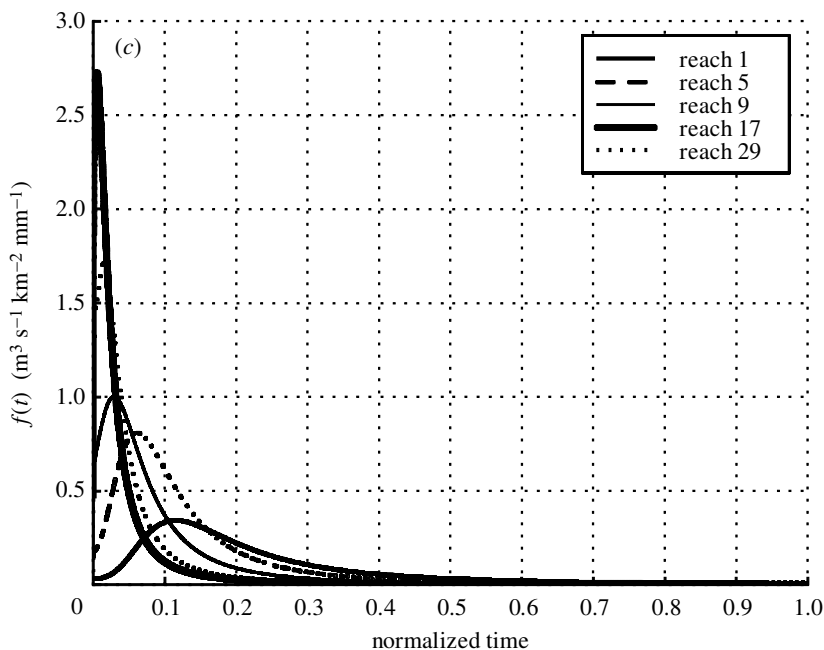


Figure 5. (Cont.) (c) Instantaneous unit response functions for reaches 1, 5, 8, 17 and 29 indicated in figure 3c.

(ii) *Space-time fields (figure 5a–c)*

Next, we use the model to gain insights into the space-time variability of the network response to instantaneous rainfall events. We do this by generating plots of the temporal variations (versus normalized time) of the average velocity v^i (figure 5a), average cross-sectional area m^i (figure 5b) and discharge $D^i = m^i \cdot v^i$ (figure 5c), for five reaches located across the network. The network of figure 3c consisting of $M = 37$ reaches is used for this purpose—the reaches selected are 1, 5, 9, 17 and 29, as indicated in figure 3c. The representative results shown are for the instantaneous event with $J = 2.5$ mm. The variations in time of the velocities and cross-sectional areas differ depending on the specific location of the reach within the network. In upstream first-order reaches, v^i and m^i always decrease in time (17 is a close approximation to this), whereas in all higher-order reaches (1, 5, 9 and 29), an initial increasing phase is followed by a decreasing phase after the flood wave from the upstream reaches has passed through. In addition, we observe, as one would expect, a spatial trend of velocity variation across the network, ranging from generally high values in the steep first-order streams to lower values in the flatter reaches close to the outlet. For a given point in time, a snapshot of v^i , m^i and D^i can be taken at different points of the network. We note that as the flood wave is travelling through, the three quantities are peaking at different locations at different times causing, at a given instant, the respective quantity to be on either an increasing or a decreasing trend at different locations. These results are at variance with assumptions of constant velocity across the network often made to advance analytical solutions of network response (see, for example, Rinaldo *et al.* 1991; Rigon *et al.* 1993). The constant velocity assumption, however, seems to become more acceptable with increasing contributing

watershed area. For example, we observe a drop in peak velocity with increasing upstream contributing area (17.17, 8.28, 3.85, 1.08 and 2.96 km², for reaches 1, 5, 9, 17 and 29, respectively). The peaks in velocity and cross-sectional area are almost in phase with the peaks of the discharge presented in figure 5c, across the network. Note that the discharges have been normalized with respect to upstream watershed areas and the depth of the event J , and hence the area under the graph is unity for all of the curves in figure 5c. Therefore, these are equivalent to the instantaneous unit hydrographs of the various sub-watersheds. However, because of the inherent nonlinearity of the responses, following Robinson *et al.* (1995), these will be called instead *instantaneous unit response functions* (IURFs). We observe that the IURFs for the five reaches are all positively skewed, while the skewness of the hydrographs and the sharpness of the peaks decrease with increasing upstream watershed area.

(iii) *Rating curves (figure 6a, b)*

We also view the same results in a different context by plotting v^i versus D^i and m^i versus D^i (the rating curve) for reach 1 (see figure 3c). We observe typical hysteresis effects in both relationships, yielding two possible values of discharge for the same velocity or cross-sectional area, the physical cause of which has been explained previously by Henderson (1966) by recourse to the momentum equation. We selected the flatter reach 1 for this purpose, as the hysteresis effects are relatively more pronounced in it than in some of the steeper upstream reaches where the hysteresis loop almost collapses into a single curve. The small near-vertical kinks in the graphs in figure 6a, b (10 mm event) are simply due to the start-up phase, i.e. the rapid transition from the steady-state initial condition to the dynamic regime dictated by the balance of forces. It is also important to note in figure 6a that the velocity changes nonlinearly with discharge during the event and becomes more flat for large near-peak values of discharge D^i , as observed by Beven (1979) and Bates & Pilgrim (1983). This flattening of the velocity increase could be even more pronounced if we had used hydraulic geometry relationships which distinguish between in-channel and over-bank (i.e. floodplain) flow regimes.

(iv) *Instantaneous unit response functions (figure 7a–c)*

We next investigate the effects of the magnitude of the rainfall inputs J and the drainage density on the response of the network, by analysing the results presented in figure 7a–c for the three networks shown in figure 3a–c. These plots present the discharge signal at the watershed outlet versus dimensionless time, with the discharge expressed in m³ s⁻¹ mm⁻¹ after being normalized by the depth of the event J (mm). It is clear that these IURFs are substantially different for the different rainfall events, even after normalizing by the rainfall depth, demonstrating a strong nonlinear response of the network. The IURFs become more peaky with increasing event size J for all three networks and are positively skewed, with the skewness decreasing as the size of the event becomes smaller. These results further confirm the empirical findings of Minshall (1960), whose work, historically, has provided the motivation for hydrologists' attempts to understand the origins of nonlinearity in watershed responses. The inherent nonlinearity of hydrological response has been

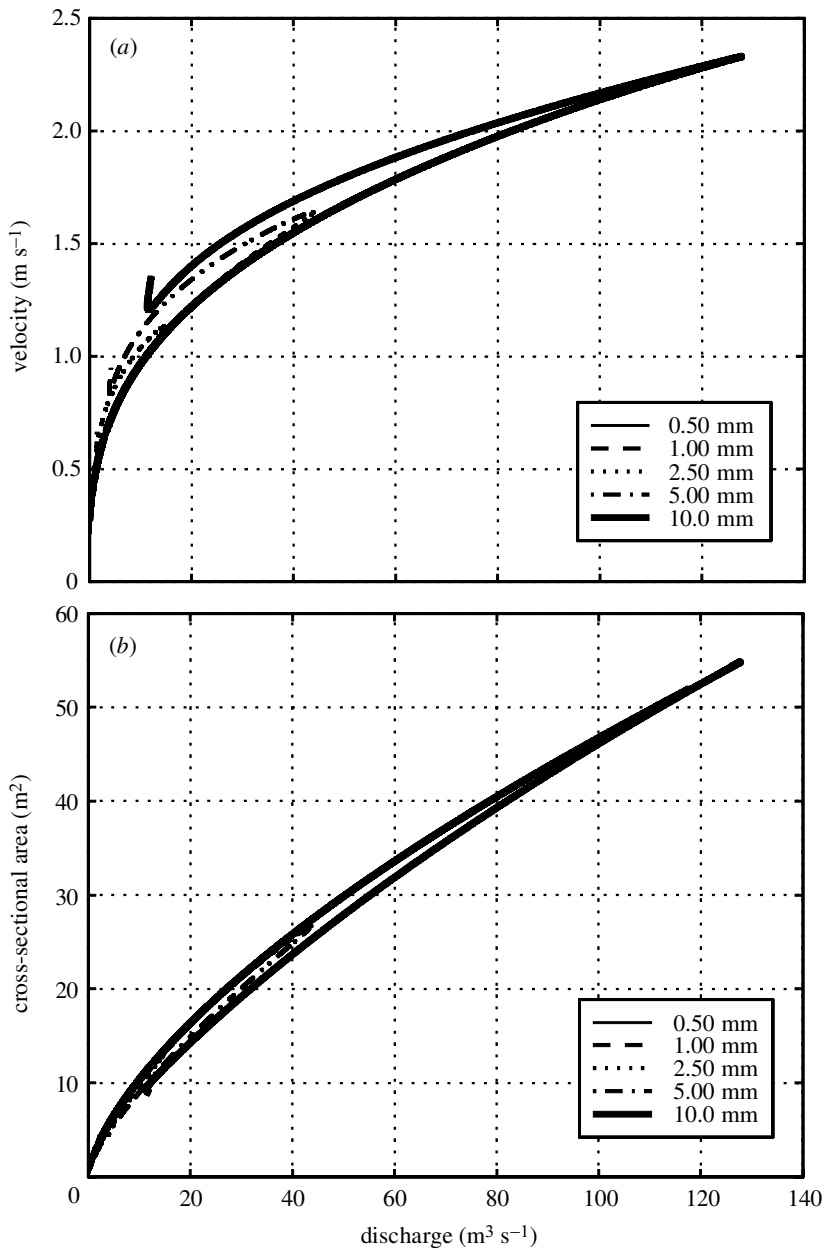


Figure 6. (a) Average velocity versus discharge for reach 1 in figure 3c.
 (b) Average cross-sectional area versus discharge for reach 1 in figure 3c.

successfully captured by Lee & Yen (1997), who proposed an analytical expression for the geomorphological unit hydrograph by estimating probabilistic distributions of travel times based on the kinematic wave theory. On the other hand, many recent network response formulations based on geomorphology (see, for example, Mesa & Miffin 1986; Rinaldo *et al.* 1991; Robinson *et al.* 1995) have, for reasons of analytical

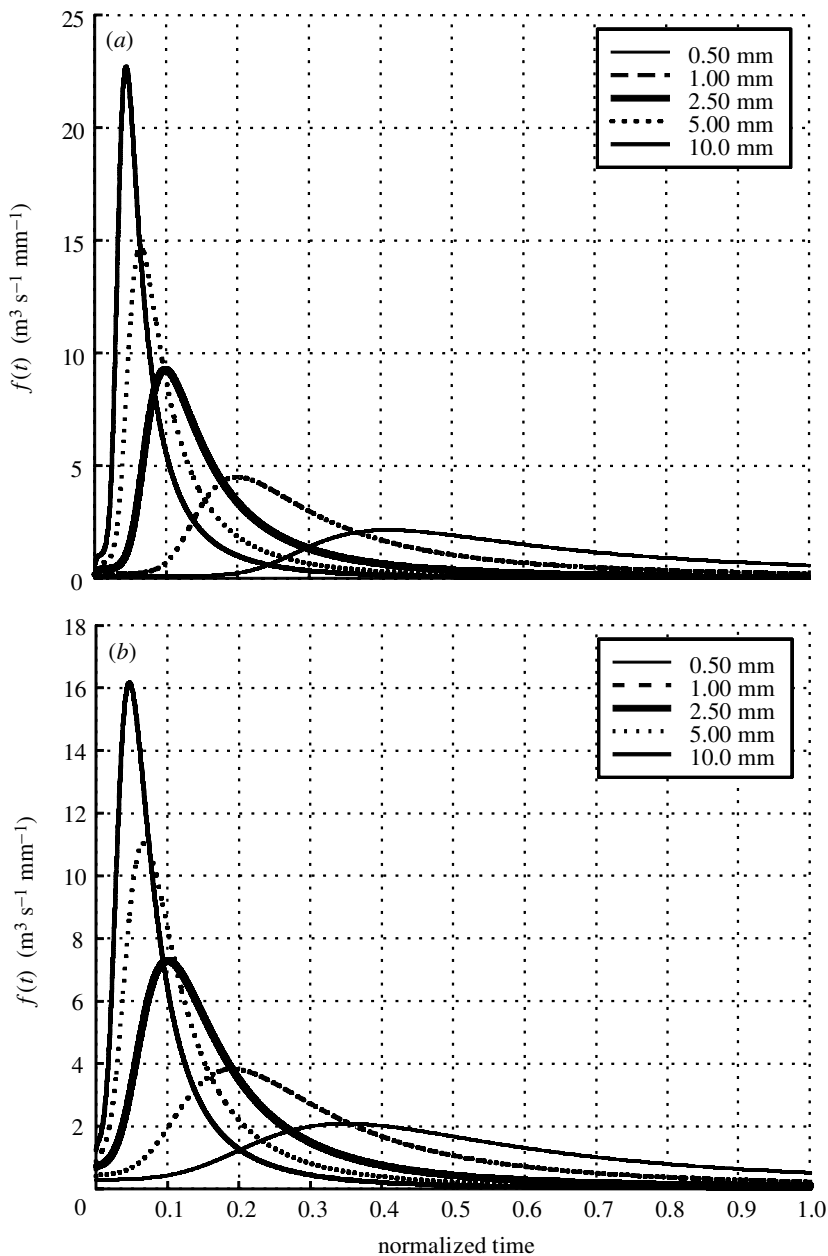


Figure 7. Instantaneous unit response functions at the outlet for the three watersheds indicated in figure 3*a-c* for five different instantaneous events.

tractability, derived IURFs of network response by convoluting the network's area or width function with a linear routing model based on constant velocity.

We can infer from the results presented above that one circumstance under which such linearity would be acceptable is when the rainfall inputs are so small that they do not change the velocity field prevailing prior to the rainfall injection. In such a

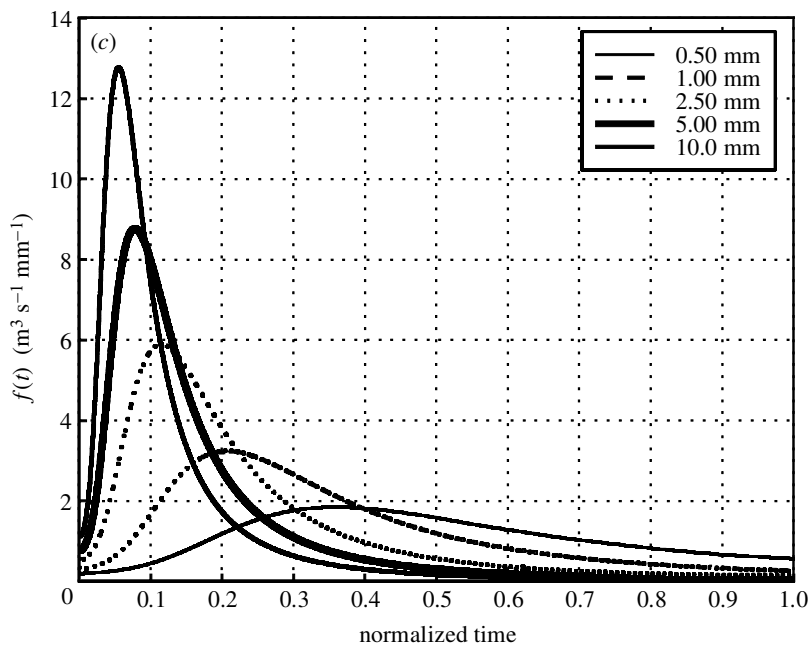


Figure 7. (*Cont.*) For description see opposite.

case, the IURF would almost be a scaled version of the underlying area function of the network (distance scaled by constant velocity to give time of travel). The area function, however, is usually negatively skewed, as shown, for example, by Rinaldo *et al.* (1995). Our results thus provide evidence that one of the reasons that empirically estimated IURFs (or instantaneous unit hydrographs (IUHs)) are positively skewed while the underlying area or width function is negatively skewed is the nonlinearity of the network response itself, dictated by the balance of forces, and modulated by hydraulic geometry.

We now attempt to explain the inherent nonlinearity of the network response by considering the balance of forces acting on the water within the reaches. Gravity and bed friction constitute two opposing forces acting on the water body. Gravitational force scales linearly with the storage of water m^i (initially dictated by the size of the event), while the frictional force is proportional to the bed area of the channel reach and the square of the velocity. The bed area is a product of the wetted perimeter P^i and the total channel length l^i . The wetted perimeter scales nonlinearly with storage due to the adopted hydraulic geometry relationships. Under non-steady conditions, the friction force, which is a second-order function of velocity, needs to rise (by acceleration) in order to balance the gravitational force. This increase in velocity is more significant in the (steeper, shallower and narrower) channels of the upper reaches than in the (flatter, deeper and wider) channels of the lower reaches. Other things being equal, the velocity thus tends to decrease as we move from the upper reaches towards the outlet. We also observe a discrepancy between the velocity predicted by hydraulic geometry relationships, which suggests a general increase of velocity towards the outlet, while the computed velocities exhibit the opposite tendency. This effect can be explained by the fact that the hydraulic geometries are

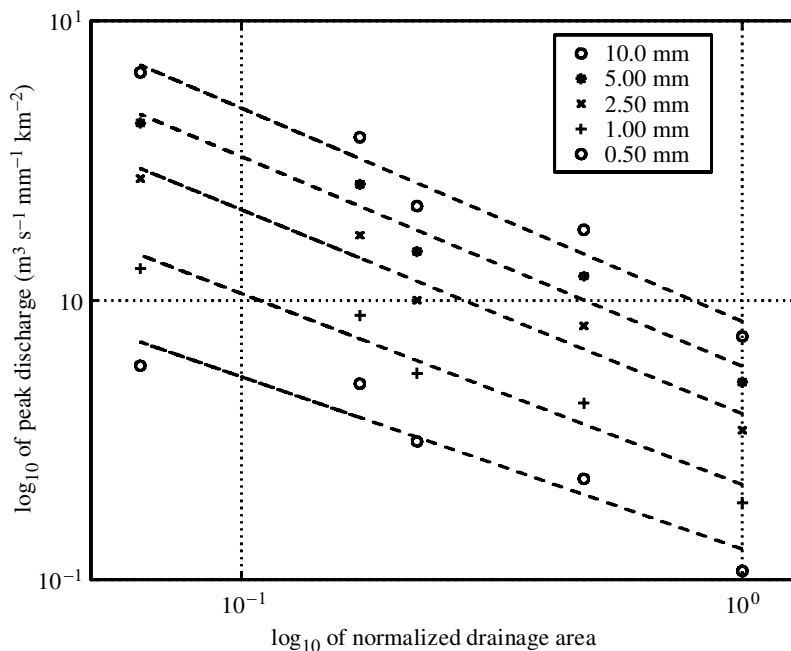


Figure 8. Peak discharge versus upstream drainage area for reaches 1, 5, 9, 17 and 29 indicated in figure 3c and five different instantaneous events.

based on steady-state assumptions, while we are modelling a non-steady dynamic situation.

The above discussion applies when drainage intensity remains constant. However, if the same volume of water is injected into a network with a higher drainage intensity, because of the inclusion of new steeper channels, the velocity distribution increases such that it is on average larger than before, while also exhibiting a slightly larger spatial distribution. Hence the steepening of the hydrograph, and the resulting non-linearity, would be larger than before. This can be confirmed by the results shown in figure 7a–c with different drainage densities.

(v) *Flood peak scaling (figure 8)*

To gain further insights into this space-time variability, and to understand the role of watershed size on flood peak scaling, we present the variations of the flood peaks, for each storm, as a function of watershed area. These are presented in figure 8 for the network shown in figure 3c. We present log–log plots (power-law relationships) of the peak flood discharges in the five reaches (1, 5, 9, 17 and 29) (normalized by the upstream contributing areas and by the depth of the event) versus the non-dimensionalized contributing area (normalized by total watershed area) for the five instantaneous events. We obtain roughly constant scaling exponents varying from -0.61 for the smaller 0.5 mm event to -0.77 for the 10 mm event. This shows a clear, albeit small, impact of nonlinearity on the scaling of the flood peaks with drainage area. With increasing event depth J , the scaling exponents seem to decrease, shifting from the scaling exponent of -0.5 which would have been observed

for a linear network response (applicable, implicitly, under rainfall depths so small that velocities remain constant), as demonstrated by Gupta & Waymire (1998) and Robinson & Sivapalan (1997).

7. Conclusions

This paper forms a contribution towards the development of a hydrologic theory applicable directly at the scale of the watershed. It focuses, in particular, on the response of a network of stream channels. The description of the theory for a more general problem encompassing other elements of a network-hill-slope system is presented in detail in Reggiani *et al.* (1998, 1999). The main contributions of the present paper can be summarized as follows.

- (1) We have presented a systematic approach for the formulation of a set of global balance laws for mass and momentum, governing the response of a stream network. The equations are stated at the spatial scale of a single reach and depend only on time. In essence, these equations constitute counterparts to the well-known Saint-Venant equations, from which space has been integrated away within individual reaches. In particular, these balance equations contain a number of unknown exchange terms for mass and forces with the surroundings and among adjacent reaches.
- (2) Estimation of these terms represents a closure problem. In this paper the closure is approached through the Coleman–Noll method, which is based on the use of the second law of thermodynamics as a constraint. The use of the Coleman–Noll method has the advantage that the constitutive relationships need not be postulated in an ad hoc manner, but are obtained naturally within a single and consistent procedure. In this fashion, common assumptions, such as dependence of the friction term on the square of the velocity and hydrostatic pressure distribution within the channel, are clearly exposed within a thermodynamic framework.
- (3) The parametrized balance equations form a set of nonlinear coupled ODEs, involving coupling between the mass and momentum equations, as well as amongst all reaches constituting the network. We have implemented a solution algorithm for the simultaneous solution of these equations based on the Runge–Kutta integration method.
- (4) The numerical model of stream network response is used to predict the space-time fields of discharge, velocity and storage for a number of instantaneous rainfall events of varying magnitude. The results are used to make inferences about the nonlinearity and scaling behaviour of the watershed responses. These are related to aspects of force balance and hydraulic geometry. We have computed the instantaneous unit response of a natural watershed (IURFs) and observed that they are strongly nonlinear in their dependence on rainfall depth. This can be attributed to nonlinear changes in bed friction and hydraulic geometry. In addition, we have also obtained empirical velocity-discharge and cross-sectional area-discharge relationships, and found these to be strongly nonlinear as well.

- (5) From the simulations we observe substantial variability of reach-average velocities both in space and in time across the network, in contrast to the assumption of near constant velocity which is often assumed for estimating watershed response during storm events.
- (6) The model results were also used, in a preliminary manner, to determine scaling relationships between flood peaks and contributing catchment area, and these too reflect strongly the effects of nonlinearity.

Since the results presented were exclusively for the stream network, it has not been possible to compare the results against observed data. Before this can happen, we would need to develop equivalent models of hill-slope response to rainfall events. This work is currently under way, based on governing equations derived in a similar manner by Reggiani *et al.* (1998, 1999). Early developments in this regard are presented in Reggiani *et al.* (2000).

The simulations we have carried out were for a steep watershed. Backwater effects are not important in this case and were not considered. The model can easily incorporate these in flat regions by the use of appropriate boundary conditions at the watershed outlet. This is left for future applications. The model also used regionalized hydraulic geometries based on Leopold & Maddock-type relationships. Applications using measured actual hydraulic geometries, including the effects of floodplains, are also worthy of further work. Finally, we propose to use the network model with spatially variable rainfall events of finite duration to investigate the scaling behaviour of the resulting flood peaks, and in this way investigate the interactions between rainfall duration and variability and network response, and the role of nonlinearity in these interactions.

P.R. was supported by an Overseas Postgraduate Research Scholarship (OPRS) offered by the Department of Employment, Education and Training of Australia and by a University of Western Australia Postgraduate Award (UPA). W.G.G. was supported by the Gledden Senior Visiting Fellowship of the University of Western Australia while on sabbatical leave at the Centre for Water Research, reference no. ED 1266 PR.

Appendix A. Derivation of the balance laws

In this appendix we describe the process of obtaining global balance laws for a single reach connecting two internal nodes within the network. The water in the reach can exchange a thermodynamic property (i.e. mass, momentum, energy or entropy) with the atmosphere across the channel's free surface, with the underlying soil across the channel bed, with the upstream reaches converging at the inlet and with the downstream reach following at the outlet. The geometric properties inherent to the channel at a cross-section are the width of the free surface w , the wetted perimeter P and the cross-sectional area m normal to the spatial curve C^i forming the axis of the channel of the i th reach, as shown in figure 2. The volume V^i associated with the reach is slender and can be approximated through the integration

$$V^i = \int_{C^i} m \, dC = m^i l^i, \quad (\text{A } 1)$$

where dC is an infinitesimal segment of C^i , while m^i and l^i are the average cross-sectional area and length of the i th reach. By making this approximation, the effects

Table 2. Summary of the properties in the conservation equations

surface	superscripts	nomenclature	parametrization
free surface	i top	$A^{i \text{ top}}$	$w^i l^i$
bed surface	i bed	$A^{i \text{ bed}}$	$P^i l^i$
end sections	ik	A^{ik}	$\frac{1}{2}(m^i + m^k)$
watershed outlet	i ext	$A^{i \text{ ext}}$	$\frac{1}{2}(m^i + m^{\text{ext}})$

of volume distortion due to curvature of the channel have been neglected. We state a generic conservation equation for a thermodynamic property ψ , as pursued by Eringen (1980), in a general form,

$$\frac{d}{dt} \int_{V^i} \rho \psi \, dV + \sum_j \int_{A^{ij}} \mathbf{n}^{ij} \cdot [\rho(\mathbf{v} - \mathbf{w}^{ij})\psi - \mathbf{i}] \, dA - \int_{V^i} \rho f \, dV = \int_{V^i} \rho \Gamma \, dV, \quad j = k, \text{ bed, top}, \quad (\text{A } 2)$$

where f is the external supply of the thermodynamic property ψ , Γ is its rate of production per unit mass, ρ is the mass density of water, A^{ij} are the various surfaces delimiting the reach (as listed in table 2), \mathbf{v} is the water velocity, \mathbf{w} is the velocity of a boundary surface and \mathbf{n}^{ij} are the various normals to the surfaces A^{ij} , pointing outwards.

Next, we give definitions for the averages of various quantities over the i th reach:

$$\psi^i \int_{V^i} \rho \, dV = \int_{V^i} \rho \psi \, dV \quad (\text{A } 3)$$

is the mass-weighted average for the thermodynamic property ψ , and

$$f^i V^i = \int_{V^i} f \, dV \quad (\text{A } 4)$$

is the volume average for the external supply term f . Definitions of the volume averaged mass density ρ^i and net production rate Γ^i are similar to that given for f^i (A 4). By adopting these definitions and using (A 1), we can rewrite the first term of (A 2) as

$$\frac{d}{dt} \int_{V^i} \rho \psi \, dV = \frac{d(V^i \rho^i \psi)}{dt}. \quad (\text{A } 5)$$

To obtain specific balance equations for mass, momentum, energy and entropy, the corresponding microscopic quantities indicated in table 3 need to be substituted into (A 2). The quantities indicated in table 3 need to be interpreted as follows: \mathbf{t} is the point-scale stress tensor, E is the internal energy, \mathbf{g} is the gravity, \mathbf{q} is the heat vector, h is the external supply of energy, η is the microscopic energy, \mathbf{j} is the entropy flux vector, b is the external supply of entropy and L is the internal production of entropy per unit mass.

In addition, reach-scale exchange terms for momentum, pressure and viscous forces, thermal energy and entropy are introduced. These quantities have been accurately

Table 3. Summary of the properties in the conservation equations

balance equation	ψ	\mathbf{i}	f	Γ
mass	1	0	0	0
linear momentum	\mathbf{v}	\mathbf{t}	\mathbf{g}	0
energy	$E + \frac{1}{2}v^2$	$\mathbf{t} \cdot \mathbf{v} + \mathbf{q}$	$\mathbf{g} \cdot \mathbf{v} + h$	0
entropy	η	\mathbf{j}	b	L

defined on a case-by-case basis in Reggiani *et al.* (1998). Their introduction allows us to express the specific balance equations in a more concise form. Furthermore, these exchange terms constitute unknown quantities of the problem, for which constitutive relationships need to be sought. The following paragraphs present the resulting expressions for the balance equations for mass, momentum, energy and entropy for the i th reach.

(a) Conservation of mass

The conservation of mass for the i th reach is stated as

$$\frac{d}{dt}(\rho^i V^i) = \sum_j e^{ij}, \quad j = k, \text{bed, top}, \quad (\text{A } 6)$$

where the exchange terms e^{ij} express the mass source terms for the reach across the various surfaces A^{ij} . Their general definition can be given as

$$e^{ij} = \int_{A^{ij}} \mathbf{n}^{ij} \cdot [\rho(\mathbf{w}^{ij} - \mathbf{v})] dA. \quad (\text{A } 7)$$

(b) Conservation of momentum

The appropriate microscopic quantities for the thermodynamic property ψ , the non-convective interaction \mathbf{i} , the external supply of ψ , f , and the internal production Γ , which need to be substituted into the generic balance equation (A 2), can be found in table 3. After introducing appropriate symbols for the momentum exchange terms, we obtain

$$\frac{d}{dt}(\rho^i \mathbf{v}^i V^i) = \rho^i \mathbf{g} m^i \xi^i + \sum_j e^{ij} \mathbf{v}^j + \sum_j \mathbf{T}^{ij}, \quad j = k, \text{bed, top}. \quad (\text{A } 8)$$

The reach-scale momentum exchange terms \mathbf{T}^{ij} are given by the expression

$$\mathbf{T}^{ij} = \int_{A^{ij}} \mathbf{n}^{ij} \cdot [\mathbf{t} - \rho(\mathbf{v} - \mathbf{w}^{ij})\tilde{\mathbf{v}}] dA, \quad (\text{A } 9)$$

where the microscopic stress effects, attributable to the deviations of the reach average velocity from its spatial average $\tilde{\mathbf{v}}$, have been incorporated into the momentum exchange terms.

(c) Conservation of energy

The balance equation for total energy includes the sum of kinetic, internal and potential energies. The appropriate microscopic quantities ψ , \mathbf{i} , f and Γ , which need to be substituted into (A 2), are reported in table 3. For constant density systems we obtain

$$\frac{d}{dt} \{ [E^i + \frac{1}{2}(v^i)^2] \rho^i V^i \} = \sum_j e^{ij} [E^i + \frac{1}{2}(v^i)^2] + \sum_j \mathbf{T}^{ij} \cdot \mathbf{v}^i + \sum_j Q^{ij} + \rho m^i \xi^i \mathbf{g} \cdot \mathbf{v}^i + \rho^i h^i V^i, \quad j = k, \text{bed, top.} \quad (\text{A } 10)$$

The reach-scale heat exchange terms Q^{ij} are defined as

$$Q^{ij} = \int_{A^{ij}} \mathbf{n}^{ij} \cdot \{ \mathbf{q} + \mathbf{t} \cdot \tilde{\mathbf{v}} + \rho(\mathbf{w}^{ij} - \mathbf{v}) [\tilde{E} + \frac{1}{2}(\tilde{v})^2] \} dA. \quad (\text{A } 11)$$

We observe that the terms accounting for the microscopic energy attributable to fluctuations of the velocity $\tilde{\mathbf{v}}$, the internal energy \tilde{E} and the kinetic energy $\frac{1}{2}(\tilde{v})^2$ have been incorporated into the heat exchange term. The balance equation for thermal energy is obtained from (A 10) by subtracting the momentum balance multiplied by the velocity (i.e. the balance of mechanical energy),

$$\frac{d}{dt} \hat{E}^i = \sum_j e^{ij} E^i + \sum_j Q^{ij} + \rho^i h^i V^i, \quad j = k, \text{bed, top,} \quad (\text{A } 12)$$

with $\hat{E}^i = \rho^i V^i E^i$ the extensive internal energy.

(d) Balance of entropy

Finally, we obtain the balance equations for entropy. After substituting the necessary microscopic values, by observing that the internal energy generation of entropy Γ is non-zero, and introducing reach-scale entropy exchange terms, we obtain

$$\frac{d}{dt} \hat{\eta}^i = \sum_j e^{ij} \eta^i + \sum_j F^{ij} + \rho^i b^i V^i + \rho^i L^i V^i, \quad j = k, \text{bed, top,} \quad (\text{A } 13)$$

where $\hat{\eta}^i = \rho^i \eta^i V^i$, while F^{ij} is given in analogy to previous definitions,

$$F^{ij} = \int_{A^{ij}} \mathbf{n}^{ij} \cdot [\mathbf{j} - \rho(\mathbf{v} - \mathbf{w}^{ij}) \tilde{\eta}] dA, \quad (\text{A } 14)$$

and $\tilde{\eta}$ is the fluctuation of the entropy from its average over the entire reach.

(e) The second law of thermodynamics

The second law of thermodynamics states that the total production of entropy within a physical system has always to be non-negative. In the present case, the system under consideration is taken to be the entire network, formed by an ensemble of M reaches,

$$L = \sum_i \rho^i L^i V^i \geq 0. \quad (\text{A } 15)$$

The inequality will be employed as a constraint-type relationship in the derivation of constitutive relationships for the closure of the mass and momentum exchange terms in (A 6) and (A 8), as explained in Reggiani *et al.* (1999).

(f) Conditions of continuity (jump conditions)

The balance equations reported above are subject to other restrictions imposed on the exchange terms at the inlet and outlet sections where reaches come together. These restrictions (known as jump conditions) express continuity in the exchange of mass, momentum, energy and entropy among connected reaches. The continuity of mass expresses that the net transfer of water across the surface A^{ij} is continuous,

$$e^{ij} + e^{ji} = 0, \quad j = k, \text{bed, top.} \quad (\text{A } 16)$$

The sum of forces exchanged across the interface also needs to satisfy conditions of continuity. These include apparent forces attributable to the mass exchange and the total stress force attributable to viscous and pressure forces,

$$e^{ij}(\mathbf{v}^i - \mathbf{v}^j) + \mathbf{T}^{ij} + \mathbf{T}^{ji}, \quad j = k, \text{bed, top.} \quad (\text{A } 17)$$

The continuity of exchange of energy across A^{ij} requires that the transfer of internal and kinetic energy due to mass exchange, and the work of the reach-scale viscous and pressure forces, obey the following equation:

$$e_{\alpha}^{ij} \{E^i - E^j + \frac{1}{2}[(v^i)^2 - (v^j)^2]\} + \mathbf{T}^{ij} \cdot \mathbf{v}^i + \mathbf{T}^{ji} \cdot \mathbf{v}^j + Q^{ij} + Q^{ji} = 0, \quad j = k, \text{bed, top.} \quad (\text{A } 18)$$

The continuity of exchange of entropy across the interface requires satisfaction of the condition

$$e^{ij}(\eta^i - \eta^j) + F^{ij} + F^{ji} \geq 0, \quad j = k, \text{bed, top,} \quad (\text{A } 19)$$

where the inequality sign accommodates the possibility of entropy production of the interface.

Nomenclature

Latin symbols

<i>b</i>	external supply of entropy ($L^2/T^3 \text{ K}$)
\mathcal{B}	linearization parameter for the mass exchange term (M/L^3)
<i>D</i>	discharge for a reach (L^3/T)
<i>e</i>	mass exchange (M/T)
<i>E</i>	internal energy per unit mass (L^2/T^2)
<i>f</i>	external supply term for ψ
<i>F</i>	entropy exchange ($M/T^3 \text{ K}$)
<i>g</i>	the gravity vector (L/T^2)
<i>i</i>	general flux vector of ψ
<i>j</i>	microscopic non-convective entropy flux ($M/T^3 \text{ K}$)
<i>J</i>	depth of instantaneous event (L)
<i>L</i>	rate of net production of entropy ($M/LT^3 \text{ K}$)
<i>l</i>	length of a reach (L)
<i>m</i>	cross-sectional area (L^2)

M	number of reaches making up the network
\mathbf{n}^i	unit vector tangent to the channel bed of the reach i
p	water pressure (M/TL)
P	wetted perimeter (L)
\mathbf{q}	heat vector (M/T^3)
Q	energy exchange (ML^2/T^3)
R	first-order Taylor expansion coefficient for the friction force (M/T)
S	drainage area for a reach (L^2)
\mathbf{t}	microscopic stress tensor (M/T^2L)
\mathbf{T}	momentum exchange (ML/T^2)
U	second-order Taylor expansion coefficient for the friction force (M/L)
\mathbf{v}	velocity vector (L/T)
\mathbf{w}	velocity vector of the boundaries (L/T)
w	top width of a reach (L)
y	mean channel depth (L)
Y	maximum channel depth (L)
z	channel bed elevation (L)

Greek symbols

γ	bed slope angle of the reach ($-$)
Γ	production of the thermodynamic property ψ
ϵ	roughness height (L)
ζ	elevation of the centre of mass of a reach (L)
η	entropy per unit mass (L^2/T^2 K)
θ	temperature (K)
μ	chemical potential (L^2/T)
ϕ	gravitational potential (L^2/T^2)
ξ	Darcy–Weisbach friction factor (L)
ρ	water mass density (M/L^3)
τ_0	channel bottom shear stress (M/T^2L)
ψ	generic thermodynamic property

References

- Band, L. E. 1986 Topographic partition of watersheds with digital elevation models. *Water Resources Res.* **22**, 15–24.
- Batchelor, G. K. 1988 *An introduction to fluid mechanics*. Cambridge University Press.
- Bates, B. C. & Pilgrim, D. H. 1983 Investigation of storage-discharge relations for river reaches and runoff routing models. *Civil Engng Trans. Inst. Engng Aust.* **25**, 153–161.
- Beven, K. 1979 On the generalized kinematic routing method. *Water Resources Res.* **15**, 1238–1242.
- Bray, D. I. 1979 Estimating average velocity in gravel-bed rivers. *J. Hydr. Div. ASCE* **105**, 1103–1122.

- Cash, J. R. & Karp, A. H. 1990 *ACM transactions on mathematical software*, vol. 16, pp. 201–222. New York: Association for Computing Machinery.
- Chow, V. T., Maidment, D. R. & Mays, L. W. 1988 *Applied hydrology*. McGraw-Hill.
- Coleman, B. D. & Noll, W. 1963 The thermodynamics of elastic materials with heat conduction and viscosity. *Arch. Ration. Mech. Analysis* **13**, 168–178.
- Cunge, J. A., Holly Jr, F. M. & Verwey, A. 1980 *Practical aspects of computational river hydraulics*. Boston, MA: Pitman.
- Eagleson, P. S. 1970 *Dynamic hydrology*. McGraw-Hill.
- Eringen, A. C. 1980 *Mechanics of continua*, 2nd edn. Huntington, NY: Krieger.
- Gray, W. G. & Hassanizadeh, S. M. 1991 Unsaturated flow theory including interfacial phenomena. *Water Resources Res.* **27**, 1855–1863.
- Gray, W. G., Leijnse, A., Kolar, R. L. & Blain, C. A. 1993 *Mathematical tools for changing spatial scales in the analysis of physical systems*. Boca Raton, FL: Chemical Rubber Company.
- Gupta, V. K. & Waymire, E. 1998 Spatial variability and scale invariance in hydrological regionalization. In *Scale invariance and scale dependence in hydrology* (ed. G. Sposito). Cambridge University Press.
- Hack, J. T. 1957 Studies of longitudinal stream profiles in Virginia and Maryland. US Geological Survey Professional Paper, no. 294B, pp. 45–81.
- Hassanizadeh, S. M. & Gray, W. G. 1990 Mechanics and thermodynamics of multiphase flow in porous media including interphase boundaries. *Adv. Water Resources* **13**, 169–186.
- Henderson, F. M. 1966 *Open channel flow*. New York: Macmillan.
- Keulegan, G. H. 1938 Laws of turbulent flow in open channels. *J. Res. National Bureau Standards* **21**, 707–741.
- Lee, K. T. & Yen, B. C. 1997 Geomorphology and kinematic-wave-based hydrograph derivation. *J. Hydraulic Engng* **123**, 73–80.
- Leopold, L. B. & Maddock, T. 1953 The hydraulic geometry of stream channels and some physiographic implications. US Geological Survey Professional Paper, no. 252, pp. 9–16.
- Mesa, O. J. & Mifflin, E. R. 1986 On the relative role of hillslope and network geometry in hydrologic response. In *Scale problems in hydrology* (ed. V. K. Gupta, I. Rodriguez-Iturbe & E. F. Wood), ch. 1, pp. 1–17. Dordrecht: Reidel.
- Minshall, N. E. 1960 Predicting storm runoff on small experimental watersheds. *J. Hydraul. Div. Am. Soc. Civ. Engng* **86**, 28–33.
- Mosley, M. P. 1992 River morphology. In *Waters of New Zealand* (ed. M. P. Mosley), ch. 16, pp. 285–304. Wellington: New Zealand Hydrological Society.
- Naden, P., Broadhurst, P., Tauveron, N. & Walker, A. 1999 River routing at the continental scale: use of globally available data and an *a priori* method of parameter estimation. *Hydrology Earth System Sci.* **3**, 109–124.
- O’Callaghan, J. F. & Mark, D. M. 1984 The extraction of drainage networks from digital elevation data. *Computer Vision Graphics Image Processing* **28**, 323–344.
- Press, W. H., Teukolsky, S. A., Vetterling, W. T. & Flannery, B. P. 1992 *Numerical recipes in C*. Cambridge University Press.
- Prigogine, I. 1967 *Introduction to thermodynamics of irreversible processes*, 3rd edn. Wiley.
- Reggiani, P., Sivapalan, M. & Hassanizadeh, S. M. 1998 A unifying framework for watershed thermodynamics: balance equations for mass, momentum, energy and entropy, and the second law of thermodynamics. *Adv. Water Resources* **22**, 367–398.
- Reggiani, P., Hassanizadeh, S. M., Sivapalan, M. & Gray, W. G. 1999 A unifying framework for watershed thermodynamics: constitutive relationships. *Adv. Water Resources* **23**, 15–39.
- Reggiani, P., Sivapalan, M. & Hassanizadeh, S. M. 2000 Conservation equations governing hillslope responses: exploring the physical basis of water balance. *Water Resources Res.* **36**, 1845–1864.

- Rigon, R., Rinaldo, A., Rodriguez-Iturbe, I., Bras, R. L. & Ijjasz-Vasquez, E. 1993 Optimal channel networks: a framework for the study of river basin morphology. *Water Resources Res.* **29**, 1635–1646.
- Rinaldo, A., Marani, A. & Rigon, R. 1991 Geomorphological dispersion. *Water Resources Res.* **27**, 513–525.
- Rinaldo, A., Vogel, G. K., Rigon, R. & Rodriguez-Iturbe, I. 1995 Can one gauge the shape of a basin? *Water Resources Res.* **31**, 1119–1127.
- Robinson, J. S. & Sivapalan, M. 1997 An investigation into the physical causes of scaling and heterogeneity of regional flood frequency. *Water Resources Res.* **33**, 1045–1059.
- Robinson, J. S., Sivapalan, M. & Snell, J. D. 1995 On the relative roles of hillslope processes, channel routing and network geomorphology in the hydrologic response of natural catchments. *Water Resources Res.* **31**, 3089–3101.
- Snell, J. D. 1996 A physically based representation of channel network response, pp. 1–247. PhD thesis, Centre for Water Research, University of Western Australia.
- Snell, J. D. & Sivapalan, M. 1995 Application of the meta-channel concept: construction of the meta-channel hydraulic geometry for a natural catchment. In *Scale issues in hydrological modelling* (ed. J. D. Kalma & M. Sivapalan), pp. 241–261. Wiley.
- Strahler, A. N. 1964 Quantitative geomorphology of drainage basins and channel networks. In *Handbook of hydrology* (ed. V. T. Chow), ch. 4-II, pp. 39–76. McGraw-Hill.